Conductive Polymeric Binder for Lithium-Ion Battery Anode

by

Tianxiang Gao

A Thesis Presented in Partial Fulfillment
of the Requirements for the Degree
Master of Science

Approved April 2015 by the
Graduate Supervisory Committee:

Ximin He, Chair
Karl Sieradzki
Candace K. Chan

ARIZONA STATE UNIVERSITY

May 2015

ABSTRACT

Tin (Sn) has a high-specific capacity (993 $mAhg^{-1}$) as an anode material for Li-ion batteries. To overcome the poor cycling performance issue caused by its large volume expansion and pulverization during the charging and discharging process, many researchers put efforts into it. Most of the strategies are through nanostructured material design and introducing conductive polymer binders that serve as matrix of the active material in anode. This thesis aims for developing a novel method for preparing the anode to improve the capacity retention rate. This would require the anode to have high electrical conductivity, high ionic conductivity, and good mechanical properties, especially elasticity. Here the incorporation of a conducting polymer and a conductive hydrogel in Sn-based anodes using a one-step electrochemical deposition via a 3-electrode cell method is reported: the Sn particles and conductive component can be electrochemically synthesized and simultaneously deposited into a hybrid thin film onto the working electrode directly forming the anode. A well-defined three dimensional network structure consisting of Sn nanoparticles coated by conducting polymers is achieved. Such a conductive polymer-hydrogel network has multiple advantageous features: meshporous polymeric structure can offer the pathway for lithium ion transfer between the anode and electrolyte; the continuous electrically conductive polypyrrole network, with the electrostatic interaction with elastic, porous hydrogel, poly (2-acrylamido-2-methyl-1-propanesulfonic acid-co-acrylonitrile) (PAMPS) as both the crosslinker and doping anion for polypyrrole (PPy) can decrease the volume expansion by creating porous scaffold and softening the system itself. Furthermore, by increasing the amount of PAMPS and creating an interval can improve the cycling performance, resulting in improved capacity retention about 80% after 20 cycles, compared with only 54% of that of the control sample without PAMPS. The cycle is performed under current of 0.1 C.

ACKNOWLEDGMENTS

I appreciate people who have made my study at Arizona State University both productive and enjoyable. I thank my family and friends for their support and love, without which I could not have finished this dissertation.

I am sincerely grateful to my advisor Dr. Ximin He, for her patient, intellectual and professional guidance and her care for my research. My work also would not have been completed without close collaboration with Dr. Ying Li, Dr. Zhi Zhao, Hanqing Han, Meng Wang, Hamsini Gopalakrishna, Jinhe Liu, Maritza Mujica, Maya Castro, and Yuwei Ling.

TABLE OF CONTENT

Page

List of Figures

Figure Page

Figure Page

List of Tables

Table Page

CHAPTER 1 INTRODUCTION

In decades, rechargeable solid-state batteries have drawn an ever-increasing research interest for portable electronic devices, especially lithium (Li)-ion batteries (LIBs), which provide high energy density, flexible and lightweight design, and longer lifespan than other comparable battery technologies.

A general battery consists of several electrochemical cells that are connected with each other to provide voltage and capacity to power the electronic devices. Each cell has a positive and a negative electrode respectively and they are separated by an electrolyte solution containing dissociated salts, which enables ion transfer between the two electrodes. Once the electrodes are connected from outside devices, chemical reactions in the internal chamber occur. By this function the electrons in the solution are free and driven to create current. Lithium battery actually does not contain lithium metal but lithium ion. For a traditional Li-ion battery, the component are a graphite negative electrode (anode), a non-aqueous liquid electrolyte, and a positive electrode (cathode), typically a kind of lithium metal oxides (lithium cobalt oxide and lithium manganese oxide) or lithium iron phosphate. However, the theoretical capacities are 372 $mAhg^{-1}$ and less than 200 $mAhg^{-1}$, respectively for these two kinds of electrode [1], which is extremely low. To further meet the increasing demand for high performance, the energy and power densities of LIBs need to be improved. Among several novel materials for anode, alloy-type anodes have been intensively explored due to their high capacity. For instance, Si has a high theoretical capacity of 4200 mAh g^{-1}, which is 10 times than that of commercial graphite. Besides, the discharging potential of Si, about 0.2 V with respect to Li/Li^{+}, is also lower than most of other alloy-type and metal oxide anodes [2]. However, Si anode also suffers from main challenges that are the huge volume variation during lithiation and delithiation processes, more than 300%, resulting in pulverization, low cycling efficiency, and permanent capacity losses.

To address this issue, lots of strategies and techniques are applied. The incorporation of materials that contain excellent conductivity and can help reduces the volume expansion. Si nanoparticles, carbon nanotubes, conducting polymers, as well as novel conductive hydrogels are promising candidates. For instance, electrically conducting polymer like polypyrrole draws much attention and is used in various applications due to its intrinsic properties like mechanical properties, high electrical conductivity, etc. And there are mainly two kinds of synthesis method of conductive polymer: chemical polymerization and electrochemical deposition. In this work the method we use is electrochemical deposition via three-electrode cell, consisting of working electrode, counter electrode and reference electrode in a solution containing polymer monomer and solvent of electrolyte. The reason of using electrochemical deposition is that very thin film can be produced and it is very quick and straightforward.

Conducting polymers are not the only additives that are incorporated into the electrode system. The anode composed of active material and polypyrrole (PPy) cannot retain good cycle efficiency, due to the large volume expansion. So several work concerning conductive hydrogels are introduced to facilitate this field. Robert Langer's group used two kinds of high molecular weight polymer hydrogels: Polycaprolactone-block-polytetrahydrofuran-block-polyCaprolactone (PCTC), pentaerythritol ethoxylate (PEE), to be entrapped with PPy simultaneously by electrochemical deposition [3]. They can provide excellent electrical and mechanical properties, and form interpenetrating network through PPy, which is a promising structure for ion battery. Anthony Guiseppi-Elie *et al*. introduced poly(hydroxyethyl methacrylate) (PHEMA) and its derivatives with PPy in application of microelecronic devices. [4] Rebeca E. Rivero *et al.* introduced poly (2-acrylamido-2-methyl-1-propanesulfonic acid) (PAMPS) that has negative charges in the solution and can be attracted by PPy [5]. These methods are not used in improving the battery electrodes yet. Besides the application of traditional hydrogels, researchers also

focused on creating 3D network of conducting hydrogels using inorganic material. Hui Wu *et al*. introduced an in-situ polymerization of PANi and phytic acid to form a conducting hydrogel that was coated on Silicon nanoparticles [6].

This thesis mainly focuses on the electrochemical deposition of polypyrrole and Sn as active material for Lithium-ion battery, and the improvement of its electrical and mechanical properties by incorporating conducting hydrogels.

CHAPTER 2 BACKGROUND AND MOTIVATION

Content:

1. The general information of Lithium-ion battery and its evolution
2. Development of anode materials
3. Introducing conducting polymers (properties and feasibility)
4. Function of other helpful hydrogels (morphology and conductivity)

2.1. The general information of Lithium-ion battery and its evolution

Rechargeable Li-ion batteries play an important role and become main components of electrical equipment for entertainment, computing, telecommunication and portable use and meet by today's requirement. During the past decades, spectacular advancing technologies of battery cells like of Ni–MeH and Li-ion batteries have been produced. These batteries are good substitutes nowadays for the well-known Ni–Cd batteries. [1] Despite Li-ion battery being one of the most promising energy storage technologies, its current performance and understanding cannot keep pace with the progress of the information technology industry.

Typically, a battery is composed of several electrochemical cells that are connected in series or in parallel in terms of structure, to provide the voltage and capacity. Each unit cell consists of a positive and a negative electrode, known as anode and cathode, separated by an electrolyte solution, always containing dissociated salts, which enable ion transfer between the two electrodes. Once both electrodes are connected externally in an electrical device, chemical reactions occur, release free ions in the electrolyte and generate current used for purpose. There are parameters for battery that are quantified. The amount of electrical energy is expressed by either per unit of weight (W h kg^{-1}) or per unit of volume (W h l^{-1}), which is also a function of the cell potential (V) and capacity (A h kg^{-1}).

The material for positive electrode (cathode) is $LiCoO_2$. During the charging, lithium ions are deintercalated from $LiCoO_2$ host, travel through the electrolyte, and are intercalated in the graphite layers in the anode. And discharge process is vice versa. [2]

2.2. Development of anode materials

Negative electrode, which is also known as anode, has been improved during several decades. Graphite micrometer-sized particle has been a dominating choice of negative electrodes for rechargeable lithium batteries for many years.

Aiming to increase the ability to store large amounts of lithium, lithium metal alloys, Li_xM_y, have drawn great interest as high capacity anode materials in lithium-ion cells. Such alloys have specific capacities much more than that of the conventional graphite anode; for example, $Li_{4.4}Sn$ (993 $mAhg^{-1}$ and 1000 $mAhcc^{-1}$ versus 372 $mAhg^{-1}$ and 855 $mAhcm^{-3}$ for graphite), and $Li_{4.4}Si$ (4200 $mAhg^{-1}$ and 1750 $mAhcm^{-3}$) [2]. Though ideally they can provide high specific capacity, accommodating such a large amount of lithium will lead to large volume expansion that accompanies their electrochemical alloy formation. This causes the deterioration of the electrode which is the formation of cracks and pulverization, thus limiting its lifetime to only a few cycles [2]. To overcome this problem, many efforts have been devoted by researchers in the earliest trials. Replacing bulk material with nanostructured alloys is one of the potential methods [7, 8]. Narrowing the metal particles to nano-dimensions have no influence on reducing the extent of volume change, but does initiate the phase transitions that accompany alloy formation, and reduces cracking within the electrode.[9] Besides applying nano-dimensioned silicon particles, binders used for silicon nanoparticles also play a tremendously important role compared to other materials. [10, 11] In 2003, Chen *et al*. demonstrated that by replacing the traditional binder poly (vinylidene fluoride) (PVDF) with poly (vinylidene fluoride–tetrafluoroethylene–propylene) (PVDF-TFE-PP) can improve the cycling performance of silicon alloys [12]. Also Li *et al*. in 2007 reported the cycling performance of silicon

nanoparticles with binder sodium carboxymethyl cellulose (NaCMC) has much better performance than that with traditional binder PVDF [13]. Other polymer binders like pure poly (acrylic acid) (PAA) and alginate are also helping with maintaining the capacity a lot. The reason of the dramatic improvement in electrochemical performance is attributed to: first, the weak interaction between the binder and the electrolyte; second, the binder can offer excellent structure to give access of Li ions to silicon. The third one is that the binder is helpful to build a deformable and stable solid-electrolyte interface (SEI) [14].

2.3. Introduction of conducting polymers (properties and feasibility)

Conducting polymer is also one kind of promising binders for anode of Li-ion battery. Conducting polymers are unique electronic functional materials due to several electrical properties, for instance, their high π-conjugated pair, unusual conducting mechanism, and reversible redox doping/de-doping process [15]. Owing to these, conducting polymers show various promising opportunities for many applications, such as sensors, actuators, artificial muscles, supercapacitors and lithium ion batteries. This project specifically investigates the application of lithium-ion batteries.

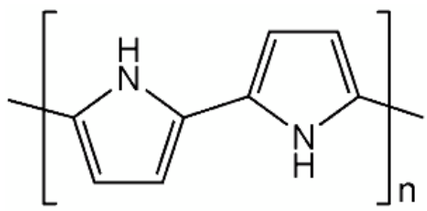

Figure 1: molecular structure of polypyrrole.

Polypyrrole is one type of conducting polymers (CPs); Figure 1 shows its molecular structure. CPs like polypyrrole can be synthesized either chemically or electrochemically. Chemical polymerization is the widely used and traditional method, typically including either condensation polymerization or addition polymerization. Lots of researchers are working on chemical polymerization of polypyrrole based on several advantages. It is feasible for larger-scale production; post-covalent modification of bulk PPy is possible as

well and there are more options to modify backbone covalently. Hui Wu *et al*. from Dr. Yi Cui's lab introduced conducting polymer, polyaniline (PANi), with phytic acid as both crosslinker and doping anion of PANi to form conformal coating that binds to the Si surface and serves as a continuous three-dimensional (3D) pathway for electronic conduction [6]. Liu *et al*. also investigated the similar in-situ polymerization of Polypyrrole, with single wall carbon tube (SWNT) to form a ternary hybrid anode for Li-ion battery [16].

Although chemical polymerization method has been widely used due to its merits, it is not easy to achieve a very thin film and the general synthesis process is relatively complicated. In comparison, electrochemical preparation is more straightforward, and the most significant difference between electrochemical and chemical synthesis is that very thin film on the order of about 20 nm can be produced directly via electrochemical deposition. Polypyrrole exhibits very promising conductivity, from 100-150 S/cm.

2.4. Function of conductive hydrogels (morphology and conductivity)

The incorporation of polypyrrole as a polymer binder for Li-ion battery does help solve the volume expansion and pulverization issue. But the results are not very good. Yongju Jung *et al*. introduced a one-step cathodic deposition method to electrochemically deposit polypyrrole and Sn particles simultaneously onto one electrode [17]. Although the method is a milestone and novel, during the battery cycling testing, after 50 cycles, the tin–PPy hybrid electrode showed capacity retention of 47%. This is a remarkable improvement compared to the performance of pure tin electrodes with a comparable thickness, which typically show a severe capacity fading within a few cycles. However, the total retention of this tin-PPy hybrid electrode is still poor compared with other works.

To try to solve the problem, many kinds of conductive polymers and hydrogels are used. Polymer hydrogels are three-dimensional polymeric networks formed from

hydrophilic monomers and polymerized to be insoluble by virtual, electrostatic or covalent crosslinking [4]. Hui Wu *et al*. and Liu *et al*. both introduced the phytic acid into the hierarchical battery system to form a 3D hydrogel [16], though phytic acid is not in the category of traditional hydrogels. Rylie A. Green *et al.* demonstrated that the key point in forming an appropriate hybrid electroconductive system is to combine the conductive and non-conductive components to preserve the overall electro-activity while enabling the desired mechanical softness and elasticity [18]. In their work, they used poly(3,4-ethylenedioxythiophene) doped with paratoluenesulfonate (PEDOT/pTS) as conducting polymers; the hydrogel part is poly(vinyl alcohol) (PVA)/ heparin methacrylate (Hep-MA) that are produced by photopolymerization. By adding the hydrogel part, the hybrids have a significantly reduced stiffness compared to pure PEDOT, showing a modulus about 2 MPa. R.G. Mahloniya *et al*. investigated an ionic hydrogel based on polyvinyl alcohol grafted with poly (2-acrylamido-2-methyl-1-propanesulfonic acid-co-acrylonitrile [19], in which poly (2-acrylamido-2-methyl-1-propanesulfonic acid) is also a good conductive hydrogel candidate.

In this project, the goal is to produce a lithium-ion battery anode by electrochemically depositing the active material (Sn) and conducting polymer (polypyrrole) and the second conductive hydrogel (PAMPS) together, to address and solve the issue of volume expansion and pulverization of Sn during the (de)lithiation process and provides good capacity retention.

CHAPTER 3 METHODOLOGY

3.1. Materials

In this project, our goal is to improve the general capacity retention during battery cycles. To investigate several important parameters, multiple samples are made, including several controls for comparison.

The main materials for experiment include:

(1) Pyrrole: monomer for polypyrrole

(2) $SnSO_4$: solvent for the reduction from Sn^{2+} to Sn particle,

(3) poly(2-acrylamido-2-methyl-1-propanesulfonic acid-co-acrylonitrile): conductive hydrogel

(4) HNO_3, $NaNO_3$: electrolyte for deposition solution

3.2. Experimental procedure

3.2.1. 3-electrode cell

The electrochemical polymerization of polypyrrole mentioned in the background section is always performed using a three-electrode configuration which typically contains a working, a counter, and a reference electrode, in a solution of the pyrrole monomer, appropriate solvent, and electrolyte. The setup is shown in Figure 2. During the electrochemical deposition, a current is passed through the solution and the deposition occurs at the positively charged working electrode or called anode. Oxidation is undergone when monomers are gathering around the working electrode surface to form radical cations that react with other monomers or radical cations. And eventually via this chain reaction they form insoluble polymer chains on the electrode surface. The total mechanism is demonstrated in Figure 3-8.

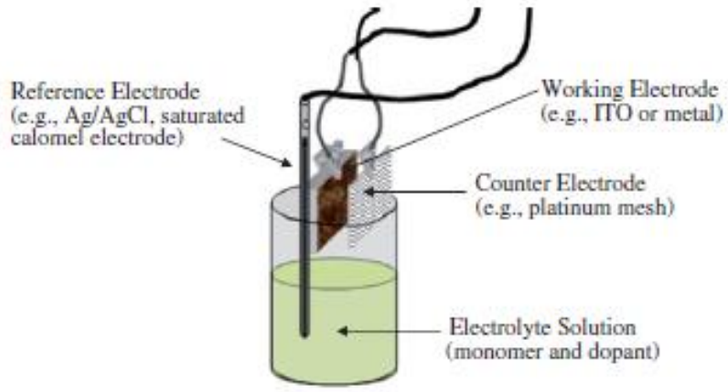

Figure 2 Schematic of a 3-electrode cell [5].

3.2.2. The electropolymerization mechanism

There is no agreement from researchers on the most accurate description of the electropolymerization mechanism. The most accepted one is Diaz's mechanism.

Step1:

The oxidation of monomer R at the surface of the electrode forms the cation radical R+•.

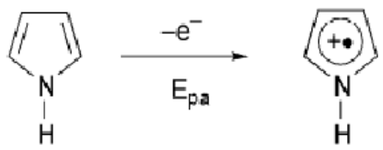

Figure 3 Chemical reaction of step 1.

Step 2:

The radical cation R+• has unpaired electron density and dimerizes with each other. The coupling between to radicals forms a bond at the α-position of each radical.

Figure 4 Chemical reaction of step 2.

Step 3:

Two protons in the α-position are lost and form the aromatic dimer.

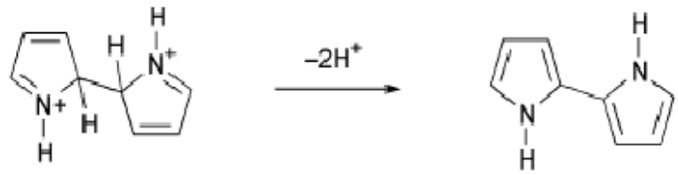

Figure 5 Chemical reaction of step 3.

Step 4:

The formation of trimer is similar with the formation of dimer.

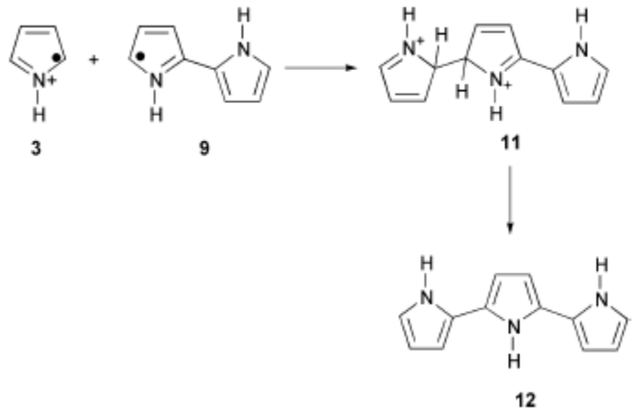

Figure 6 Chemical reaction of step 4.

Step 5:

The electro-oxidation of timer gives another radical.

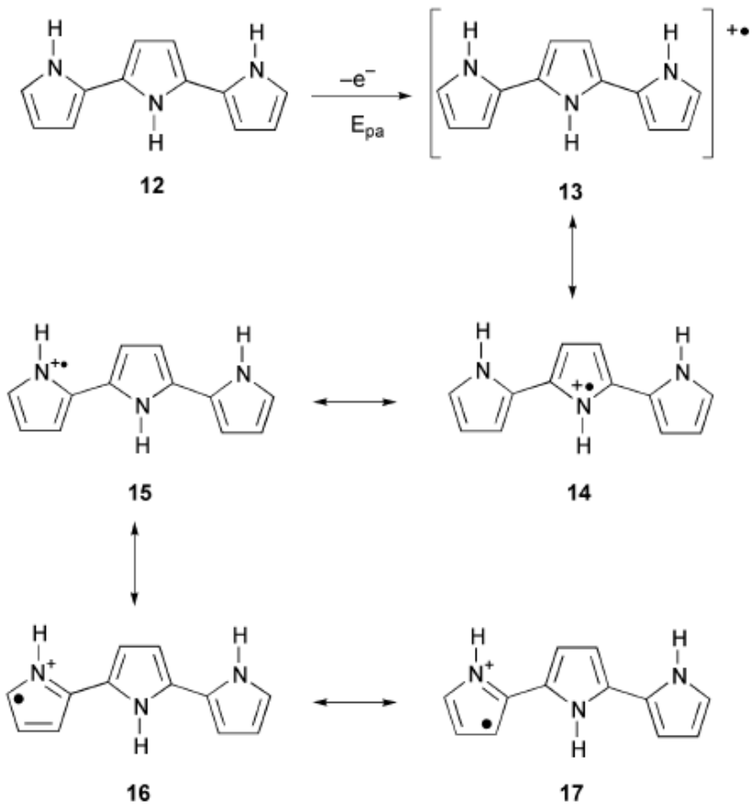

Figure 7 Chemical reaction of step 5.

Step 6:

The sequential propagation happened until the final polymer is obtained.

The electropolymerization gives an oxidized conducting form. Each 3 or 4 pyrrole units contain a positive charge and is balanced by an anion.

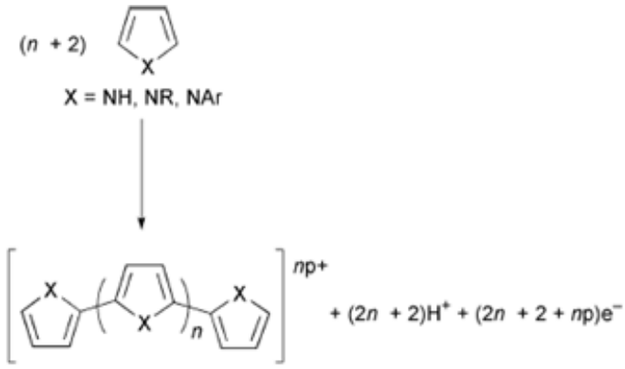

Figure 8 Chemical reaction of step 6.

3.2.3. Influences of variables on electrochemical deposition

A number of important variables have considerable effects on morphology, mechanics and conductivity. Those variables include deposition time, temperature, solvent system (water content), electrolyte, and electrode system as well as deposition charge.

(1) Effect of electrolyte

The anionic dopant represents 30% weight of the polymer film and affects the morphology and characteristics of PPy. The nature of hydrophobic character and the interaction between polymer and dopant will influence the film. Generally, higher basicity of anion leads to a lower conductivity of polymer. In a reported work, the conductivity and tensile strength will increase by 50-70% when the concentration of electrolyte increases from 0.2 M to 1 M [20].

(2) Effect of solvent

The nature of solvent should prevent the nucleophilic reaction. Similarly, the basicity is also an important factor that influences the polymer formation. Water or aqueous

solution favors the reaction by capturing the protons from the electrolyte and prevents the passivation of the electrode.

(3) Effect of pH

The pH of solution can affect the reactivity and stability of polypyrrole deposited on the electrode. Generally, acidic solution favors the polymerization. But if the solution is much more acidic, the conductivity will be compromised. It will be better if the concentration of HCl is less than 10^{-4} M [20].

(4) Effect of temperature

In general, lower deposition temperature will contribute to higher conductivity. At higher temperature, side-reactions happen and cause the formation of structural defect. Best conductive performance can be achieved by the temperature between -20 to 10 °C.

3.2.4. The simultaneous deposition

3.1.1.1.*Preparation of control sample (PPy/Sn)*

To form a metal-polymer hybrid electrode using conducting polymers as a matrix to embed or disperse metal particles, a two-step electrodeposition process is typically used to prepare samples: electropolymerization of conducting polymer followed by metal deposition. This two-step synthesis is very cumbersome, and more importantly, it limits the types and qualities of hybrid architectures that can be assembled. This is because the simultaneous electropolymerization of polypyrrole and metal deposition requires an oxidation and a reduction reaction at the working electrode, respectively, and the potential has large different range with each other. Here we refer a novel cathodic deposition of polypyrrole created by Yongju Jung *et al*. and they reported this for the first time.

The cathodic deposition of conducting polymers was achieved by combining the oxidation and reduction reactions [17]. The first reaction is the generation of an oxidizing agent, the nitrosyl ion (NO^+). The production of NO^+ ions involves reduction of nitrate

ions ($NO3^{--}$) from HNO_3 to nitrous acid (HNO_2) [Eq. (1)] [23, 24]. HNO_2 is amphoteric, which means it can generate various species depending on the difference range of pH. In this case, under strongly acidic conditions, HNO_2 reacts with H+ ions and generates the NO^+ ion [Eq. (2)], which is a strong oxidizing agent.[20-22]

$$NO3^- + 3H^+ + 2e^- = HNO_2 + H_2O \quad (1)$$

$$HNO_2 + H^+ = H_2NO_2^+ = NO^+ + H_2O \quad (2)$$

The second reaction is chemical oxidation of pyrrole by NO^+ ions and polymerization process described in the previous section that will be initiated. Since the oxidizing agents are generated at the working electrode, polymerization of PPy occurs predominantly in situ on the working electrode and eventually a thin film of hybrid system is formed onto the surface of cathode. The novel setup of the experiment is demonstrated in Figure 9. In this configuration, the working electrode is copper, the counter electrode is Pt wire and the reference electrode is Ag/AgCl 1M KCl.

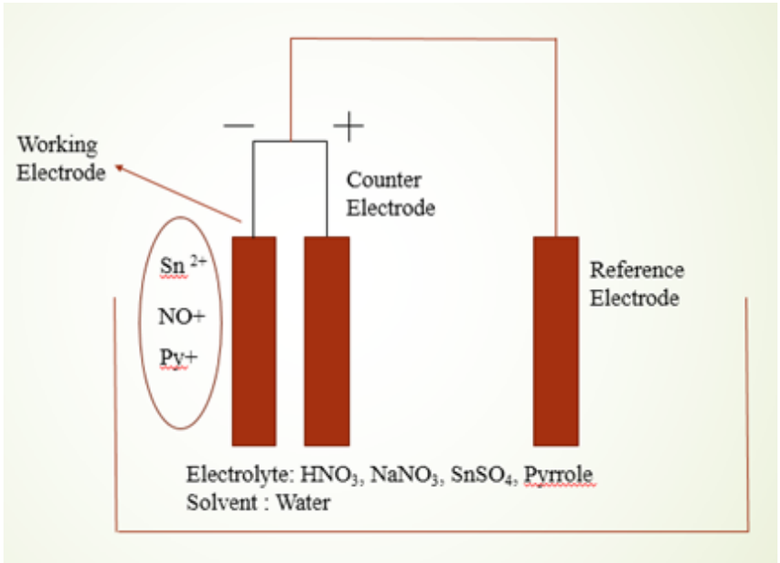

Figure 9 Cathodic EC deposition setup.

The deposition conditions include an aqueous solution containing 0.4M HNO_3, 0.5M $NaNO_3$, and 0.2M pyrrole and 0.1M $SnSO_4$. The detail of the recipe is in Table 1.

Table 1 The deposition solution ingredient details.

Chemicals	Molarity	Molecular weight	Amount	Unit

HNO_3	0.4	85	1.128	g
$NaNO_3$	0.5	63.01	1.275	g
$SnSO_4$	0.1	214.77	0.644	g
Py	0.2	67.09	0.416	ml

Electrodeposition was carried out at E= -0.65 V versus the reference electrode. Based on the influence of the condition on the deposition results, the best performance of conductivity is achieved in the range of -20 to 10 °C in terms of temperature. So the total setup is in ice bath to offer lower temperature.

3.1.1.2.Preparation of PPy/Sn/PAMPS sample

For comparison with control sample (PPy/Sn hybride), poly (2-acrylamido-2-methyl-1-propanesulfonic acid-co-acrylonitrile) aqueous solution (average Mw 2,000,000, 15 wt. % in H_2O, sigma-Aldrich) is adding into the total solution. Since the average molecular weight of PAMPS is very large compared with PPy, it is not easy to calculate and correspond their relative amount in terms of molarity, so three different (0.5g, 1.0g and 1.5g) values using gram as unit are selected. The details are shown in Table 2.

Table 2 PPy/PAMPS ratio in the solution.

1. Recipe	PPy	PAMPS
Mole/gram 1	0.25	0.5
Mole/gram 2	0.25	1
Mole/gram 3	0.25	1.5

Since the potential applied on the working electrode is negative (-0.65 V) and the PAMPS solved in the solution has anodic feature (negatively charged), so there should be an electrical repulsion between two negative part (shown in Figure 10).

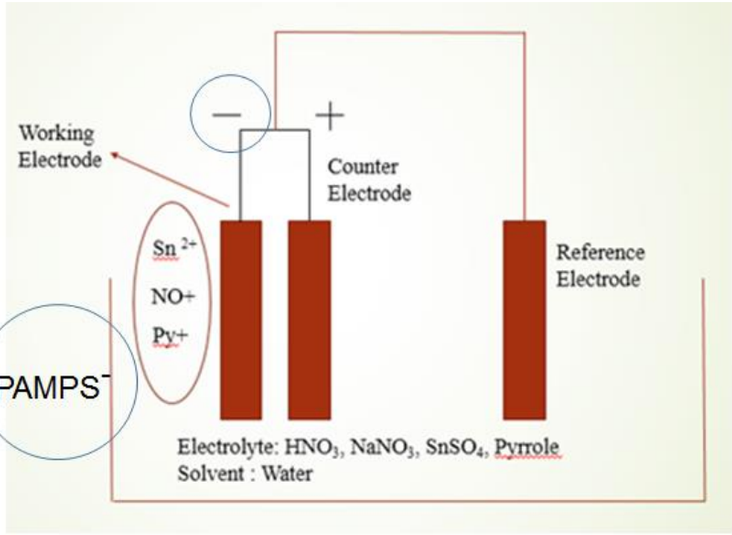

Figure 10 Schematic of batch for PPy/Sn/ PAMPS sample.

As it is not clear if the electrostatic attraction between PPy^+ and $PAMPS^-$ or the electrical repulsion between working electrode and $PAMPS^-$ will dominate, here another unique parameter is introduced: deposition/interval ratio, which means that identical short intervals will be set after a period of time of deposition. The interval is to provide sufficient time for the electrostatic attraction between PPy^+ and $PAMPS^-$, and the negative potential on working electrode will be cancelled for a while, meaning there is no repulsion to $PAMPS^-$. To investigate the influence of interval, three deposition-interval ratios are set in Table 3.

Table 3 Deposition to interval ratio detail.

Different time ratio	Deposition	Interval
1	900 s	0 s
2	50 s per cycle (18 cycles)	50 s per cycle (18 cycles)
3	25 s per cycles (36 cycles)	25 s per cycles (36 cycles)

CHAPTER 4 RESULTS AND DISCUSSION

4.1. Morphology and structure

4.1.1. SEM characterization

4.1.1.1 Control sample (PPy/Sn hybrid)

From the results of Yongju Jung's work, scanning electron microscopy (SEM) shows that their resulting PPy film contains spherical particles with diameters ranging from 50 to 200 nm. Moreover, a unique three dimensional porous network is created via this method, which creates high surface area and pathways for the transfer of lithium ion between electrolyte and anode during charging process. This is directly beneficial for a lithium ion battery. In Figure 11 (a), the structure is shown in SEM image [17].

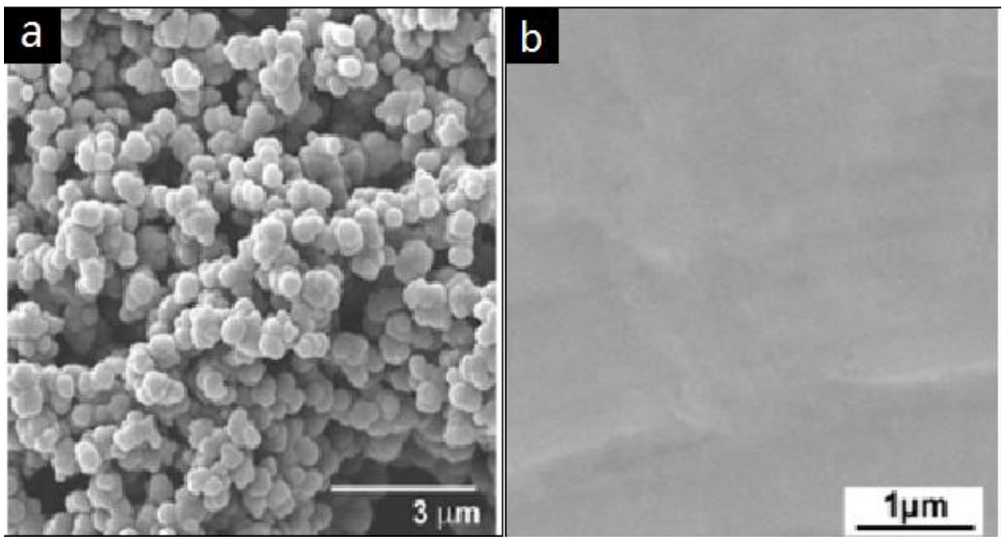

Figure 11 SEM image of a: PPy/Sn hybrid made by cathodic deposition, c: PPy made from anodic deposition. [17].

In comparison, PPy made by the traditional anodic preparations typically results in a two-dimensional planar surface morphologies. The SEM image of the PPy film deposited by applying an anodic potential (E= +0.80 V vs. Ag/AgCl) using the same solution is shown in Figure 11 (b). The particle of the film displays similar spherical features on the surface as well, but its surface is essentially two dimensional and since it is almost continuous and plain, there is even no mesoporosity.

On the other hand, the new cathodic polymerization method opens up possibility to fabricate the metal/conducting polymer hybrid electrodes through one-step deposition, because a broad range of metals can be cathodically deposited at the electrode where NO^+ can be generated as well. During this co-deposition process, a new hybrid architecture can be generated instead of the plain film made by the anodic preparation. One preliminary reason is that metal deposition and polymer deposition has different nucleation and growth mechanism, thus they will influence each other on this level. In addition, co-deposition method will also increase the uniformity and help with the distribution of metal particles within the conducting polymer matrix compared to the two-step deposition.

By characterizing our samples that made from repeating their method, we got a SEM image that indicated a very similar 3D porous architecture. There are very obvious hierarchical PPy nanospheres formed and the spheres size ranges from 20 to 500 nm. In Figure 12 (a), the image is very close to image in Figure 11 (a). Polypyrrole spheres are continuously connecting with each other to form a meshporous network. And sphere in magnified Figure 12 (c) is noticeably rough compared with pure polypyrrole, since we believe that Sn particles are dispersed uniformly onto the surface of PPy spheres, which is confirmed in Yongju Jung's work by characterized of TEM. And this phenomenon can also be proved by EDX mapping and TEM information that will be mentioned later.

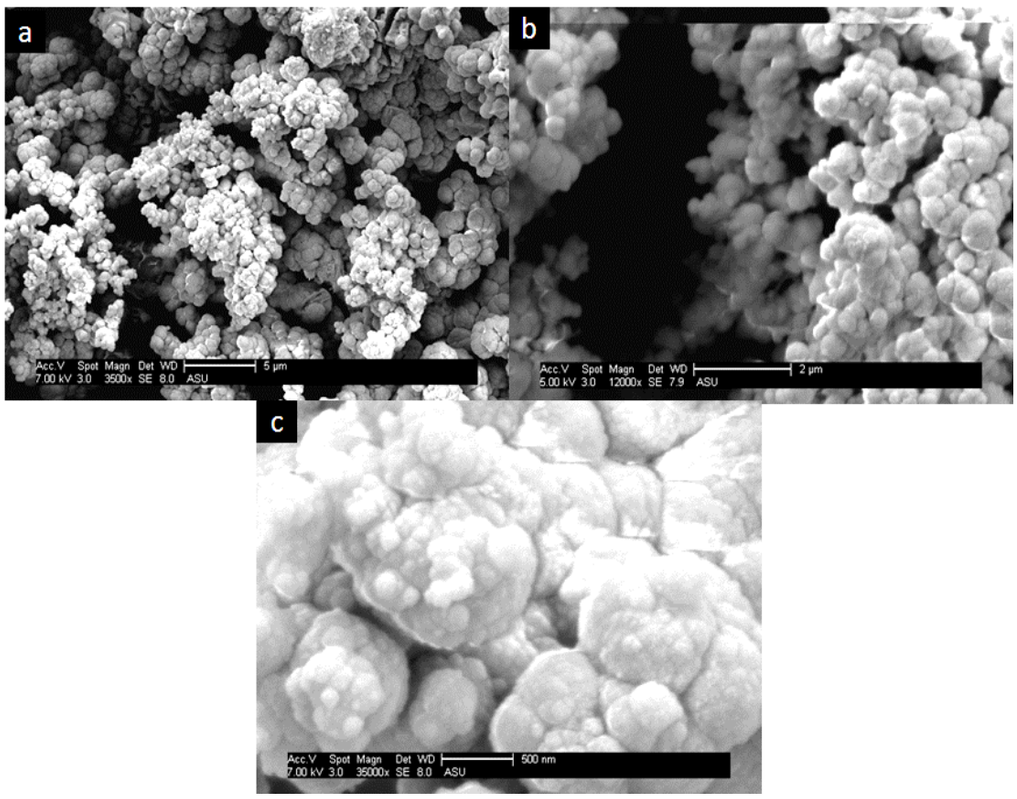

Figure 12 SEM image of PPy/Sn hybrid made by cathodic deposition, a: 3500 magnification, b: 8000 magnification, c: 35000 magnification.

In this control sample, the resulting tin-PPy hybrid morphologies are promising for improving both cycle properties and rate capabilities compared with pure Sn particle metal anode. The PPy spheres in the matrix can serve as relatively good buffer that can offer elastic flexibility to give the capacity to reduce the volume expansion of nanoparticulate of tin layers during cycling. In addition, the total coating layers of tin on a porous PPy network will enable facile Li-ion transfer and diffusion between electrolyte and anode, thus resulting in high rate capabilities. Another essential advantage of this hybrid electrode is that high weight content of tin in the anode can be successfully achieved. In this case, the as-deposited tin-PPy electrode was used directly to assemble as the Li-ion battery anode because tin particles have an excellent adhesion to the PPy spheres and continuity between the particles within the tin layers.

4.1.1.2. PPy/Sn/PAMPS samples

The difference of synthesis between PPy/Sn/PAMPS samples and PPy/Sn control samples is that PAMPS aqueous solution are added into the whole solution. And PAMPS

is supposed to serve as both crosslinker and electrostatic doping anion of PPy. The main function is to help with the PPy as an additive ingredient in the whole buffer to improve cycling performance since the control sample containing only PPy also reveals a bad cycling performance and the results will be discussed in next section.

The SEM images of PPy/Sn/PAMPS samples (in Figure 13) show a similar 3D meshporous network compared to PPy/Sn hybrid control sample. This means the supplement of PAMPS hydrogel into the system does not impair the original PPy/Sn architecture and the three-component (PPy, Sn, PAMPS) here should be formed conformally since the electrochemical deposition is processed simultaneously.

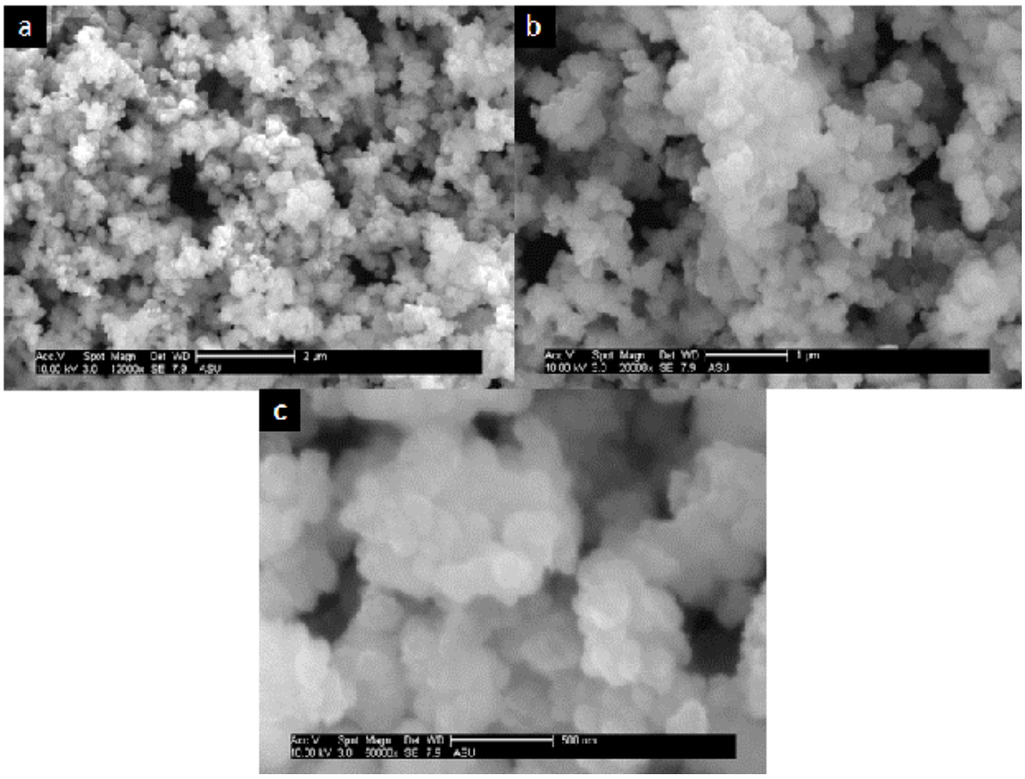

Figure 13 SEM image of PPy/Sn/PAMPS hybrid made by cathodic deposition, a: 12000 magnification, b: 20000 magnification, c: 50000 magnification.

By investigating the structure more thoroughly from b and c of high magnification, we can find that the contour line of PPy particles with each other is not very obvious compared to that of particles in PPy/Sn sample. This may be caused by the encapsulation of PAMPS onto PPy spheres. The existing form of PAMPS in the aqueous solution is anionic, accommodating with the positive charged PPy. From the comment of Rylie A.

Green *et al*. by employing an anionic hydrogel component to dope the CP component, an interpenetrating network can be formed, where both components will occupy the same space [17].

4.1.2. EDX mapping

To investigate the distribution of elements and the assumption mentioned previously about the PPy, PAMPS, Sn dispersion, EDX mapping images give straightforward information (Figure 14). It is obvious that the distribution of carbon (C), Nitrogen (N) and oxygen (O) are almost the same and all of them are corresponding to the area where relatively white PPy spheres exist. While the amount of those three elements is dramatically low in the areas where there are porous hollow parts. On the other hand, Sn is formed in the whole selected sections. This means Sn is eletrodeposited very evenly outside the thin film, thus matching the discussion that Sn is dispersed on the surface of PPy spheres. This theory can also be proved by TEM in the future. PAMPS contains C, N and O, so the distribution of these elements represents the position of PAMPS, too. And the areas of highlighted white spheres also cover the PAMPS component, meaning PAMPS and PPy occupy the same position and it is more likely forming a interpenetrating network (IPN) with each other by encapsulating the PPy sphere via their electrostatic attraction.

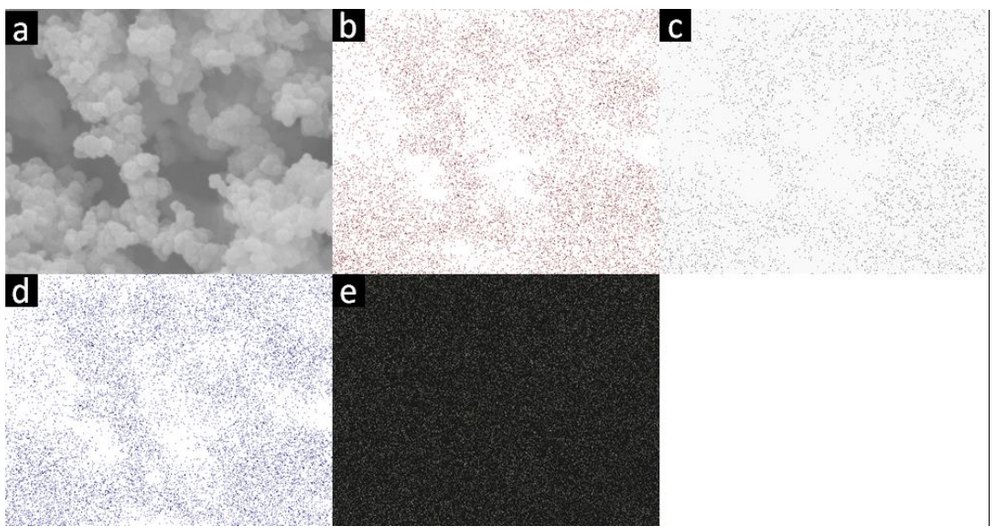

Figure 14 EDX image of PPy/Sn/PAMPS hybrid, a: selected SEM image, b: distribution of carbon c: distribution of nitrogen, d: distribution of oxygen, e: distribution of tin.

4.1.3. TEM characterization

To further investigate the structure of PPy/Sn/PAMPS samples and the interaction relationship of those three components, TEM characterization is performed (Figure 15).

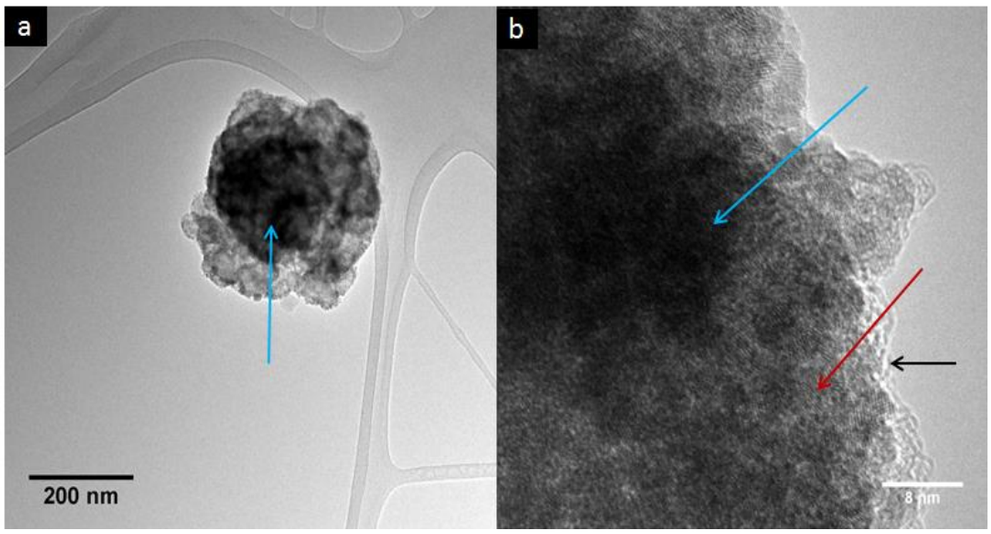

Figure 15 TEM image of PPy/Sn/PAMPS sample a: low magnification, b: high magnification, blue arrow points at PPy spheres; red arrows point at Sn crystal lattice.

In Figure 15(a), there is an intact PPy sphere containing black PPy part and the Sn and PAMPS layers outside the PPy. This is clearer in Figure 15(b) which is shown in high magnification. In Figure 15(b), blue arrow represents the PPy spheres; the red one represents the Sn layer which has crystalline lattice pattern, confirming the formation of Sn; and outside the PPy sphere there are light black regions connecting Sn lattice as well as PPy, which is the PAMPS part. The results from TEM further prove the hypothesis of the morphology of PAMPS/Sn/PPy samples mentioned in previous SEM and EDX results. And these also confirm the interactions between PPy and PAMPS and the distribution of Sn nanoparticles onto the surface of PPy.

Although the morphology is what we expected, from some other spots of TEM, the formation of PAMPS layers are not homogenous everywhere, and the thickness and

distribution are not very uniform as well. The fabrication of the hybrid system containing three components still needs optimization since the method of electrochemical deposition is every sensitive to experimental parameters, environment and human operations. To get better structure there are many challenges and issues to be investigated in the future.

4.1.4. X-ray Diffraction (XRD) characterization

To confirm during the electrodeposition, the Sn^{2+} is reduced to Sn and rather than remaining as Sn^{2+} and even oxidized into Sn^{4+} to form SnO and SnO_2, respectively, the X-ray Diffraction detection is necessary to check the exact chemical compound in the hybrid system. Although Sn, SnO and SnO_2 are all serving as the active material for lithium-ion battery anode, they have different specific capacities. And if there are mixture of them, the weight percentage of each needs to be calculated to integrate the total capacity of the electrode.

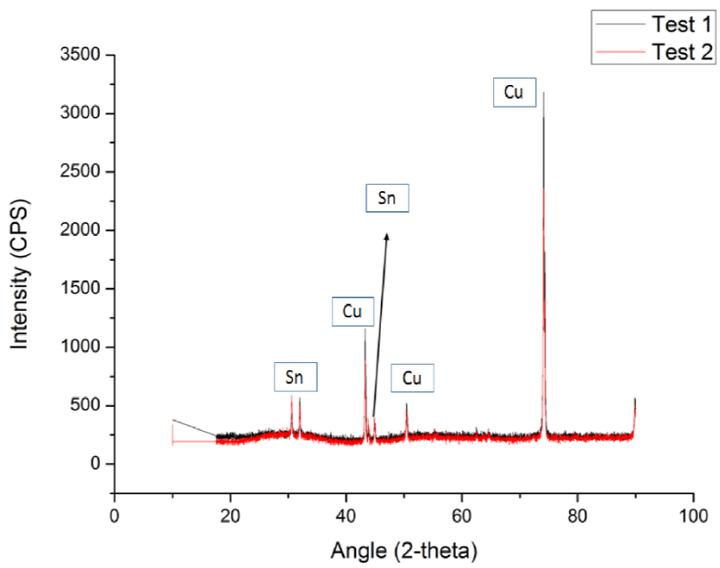

Figure 16 XRD pattern of PPy/Sn/PAMPS hybrid. (Peaks of Sn and Cu are marked).

From the XRD pattern (Figure 16), the peaks of Sn and Cu are outstanding and marked out respectively. And there is no obvious peak for SnO and SnO_2. To get better

intuitive XRD patterns of those materials, a referenced pattern of Sn, SnO and SnO_2 is also shown.

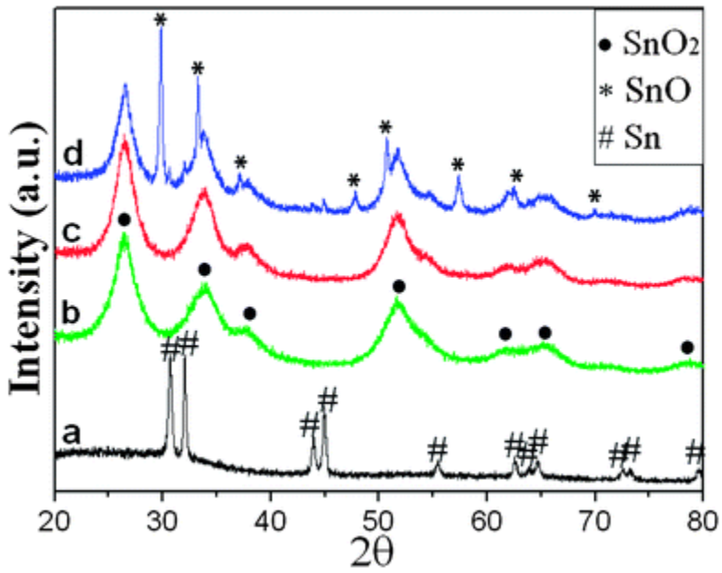

Figure 17 XRD pattern of Sn/SnO/SnO2 [27].

In Figure 17, the relative peak positions of SnO and SnO_2 are quite different of those of Sn. By corresponding the 2-theta positions with the results from experiment, there is no peak between 25°and 30°, between 35° to 40° and between 50° to 55°. It means there is no SnO and SnO_2 in the system or their amount can be neglected.

4.2. Performance of battery anode cycling retention

4.2.1. Control sample (PPy/Sn hybrid)

In Yongju Jung's work, the cycle performance of the tin-PPy hybrid electrode after 50 cycles is shown in Figure 18. They used a charging and discharging rate of 1 C during the processes. The initial capacity of the hybrid electrode is 942 $mAhg^{-1}$ of Sn. This value is approximately 2.5 times larger than that of traditional graphite anodes (ca. 330 $mAhg^{-1}$ of composite) [1], suggesting that the tin-PPy hybrid electrode is a potential candidate as anode material for future high-energy-density Li-ion batteries. The tin-PPy hybrid electrode showed a capacity retention of 47% after 50 cycles. Compared to pure tin anode, this is remarkable improvement, since tin anodes typically show a severe capacity fading within a few cycles. These results can be attributed to the unique composite structure, in

which PPy spheres provided a high surface area backbone to deposit tin thin layers, efficiently buffered the volume expansion and reduced pulverization and enhanced the cycling property of tin.

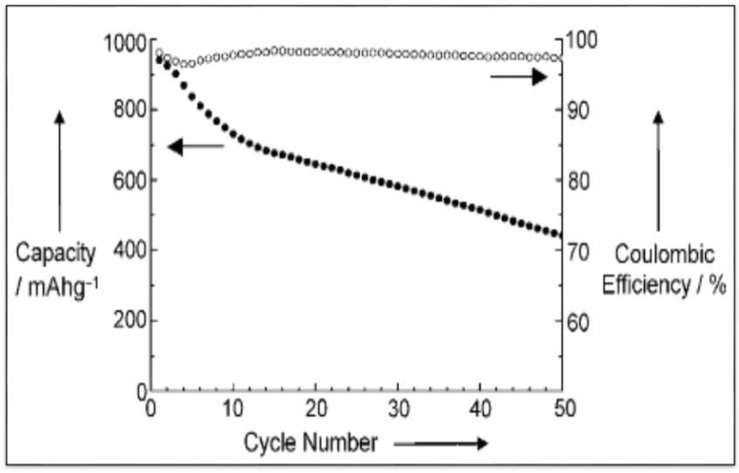

Figure 18 Cycling retention of PPy/Sn hybrid in the work of Jung, et al. [17].

The results of cycle retention of control sample (PPy/Sn) in this project are very close to those of their work, only showing a retention about 54.7% after 20 cycles (Figure 19). Although the performance is improving significantly than the pure tin electrode, generally it is still poor. The initial capacity is 923 $mAhg^{-1}$ and after 20 cycles it drop down to 506 $mAhg^{-1}$ of charge capacity and 511 $mAhg^{-1}$ of discharge capacity respectively.

4.2.2. Hydrogel/Sn/PPy sample

Many efforts has been put into overcoming the poor retention, mainly by incorporating conductive additives as binder. In Hui and Dr. Cui's work, a 3D hierarchical hydrogel network is formed conformally by in situ polymerization of PANi and the incorporation of phytic acid. Figure 20 gives a clear illustration about the molecular representation of phytic acid and the architecture of this hybrid network.

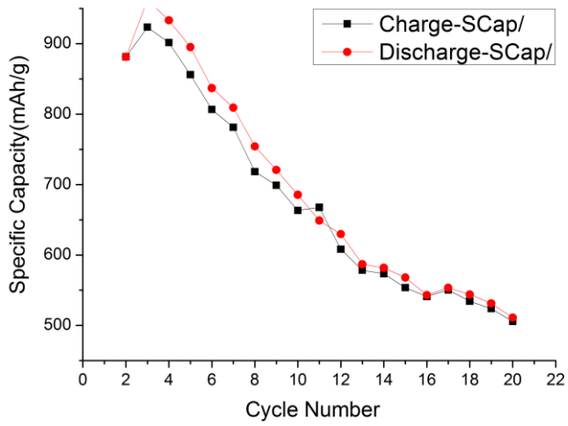

Figure 19 Cycling retention of PPy/Sn hybrid from experiment.

The phytic acid in this system is a naturally popular molecule consisting of six phosphoric acid groups. It can serve as both gelator and dopant to react with the aniline monomer by protonating the nitrogen groups on polyaniline (PANi) [25]. Phytic acid reacts with PANi by protonating the nitrogen groups on PANi. Because each phytic acid molecule can interact with several PANi chains, this crosslinking effect results in a 3D mesh-like hydrogel network.

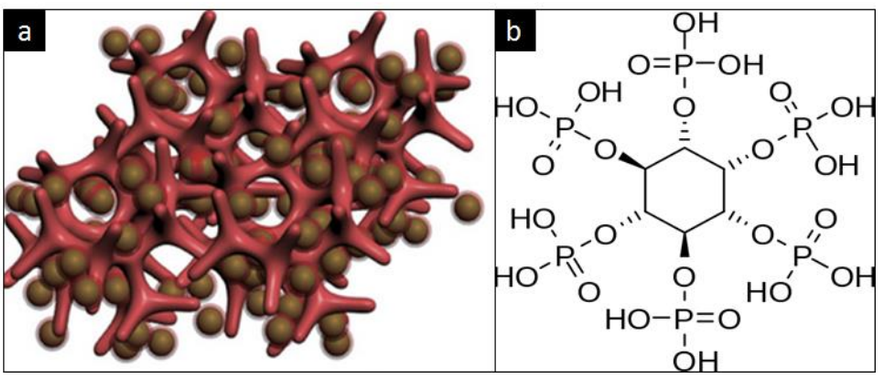

Figure 20 Schematic illustration of a: 3D porous SiNP/conductive polymer hydrogel composition electrodes, b: molecular representation of phytic acid [6].

To form a similar porous network structure that can benefit the cycle retention, this project introduces the PAMPS hydrogel, which contains the sulfuric acid group in each monomer unit. And each unit can interact with PPy unit.

To look deeper into the influence of PAMPS, several parameters are considered. The first is the amount. To distinguish the effect of amount, three different values are chosen: 0.5g, 1.0g and 1.5g. The corresponding cycling test results are shown in Figure 21. By increasing the content of PAMPS into the solution, the cycling retention keeps better. The

sample from the addition of 0.5g PAMPS has no obvious improvement compared to the control sample. While samples made from the addition of 1.0g and 1.5 g retain the retention better than that of 0.5g one. But the difference between PAMPS of 1.0g and 1.5g samples are not large. From the investigation it suggests that increasing the amount of PAMPS solution will also lead to the increasing of the PAMPS component onto the anode thin film, and eventually increase the capacity retention.

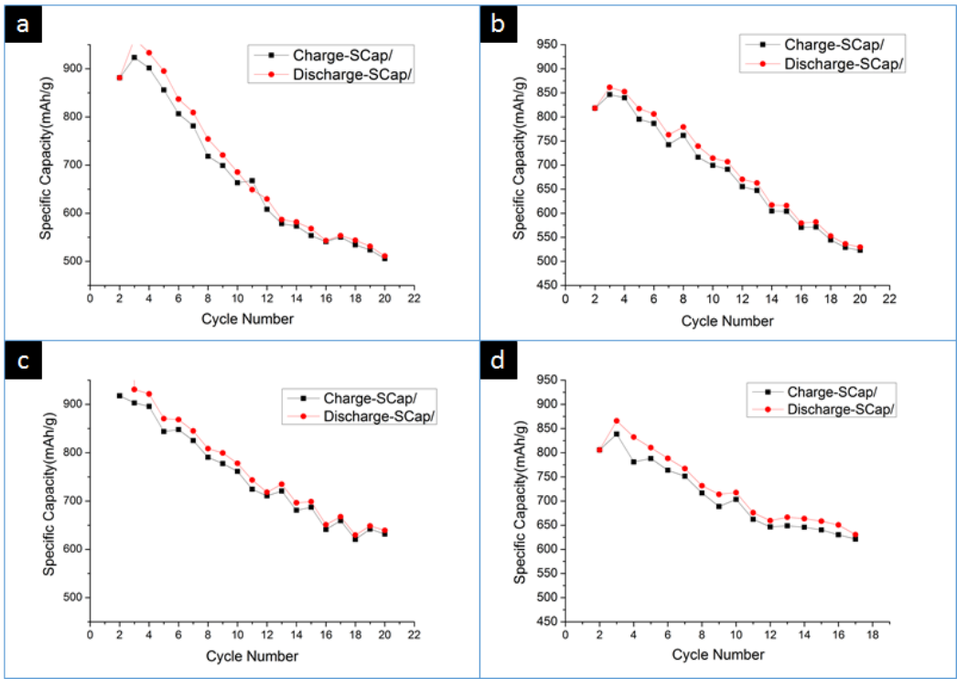

Figure 21 Cycling retention of a: control sample, b PPy/Sn/PAMPS made from 0.5g PAMPS, c: PPy/Sn/PAMPS made from 1.0g PAMPS, c: PPy/Sn/PAMPS made from 1.5g PAMPS.

To give clearer comparison of the cycling retention performances of control samples, results of PPy/Sn/PAMPS samples made from addition of 1g PAMPS solution and PPy/Sn/PAMPS samples made from addition of 1.5g PAMPS solution are demonstrated in Figure 22. It gives a more obvious illustration about the discussion in last paragraph.

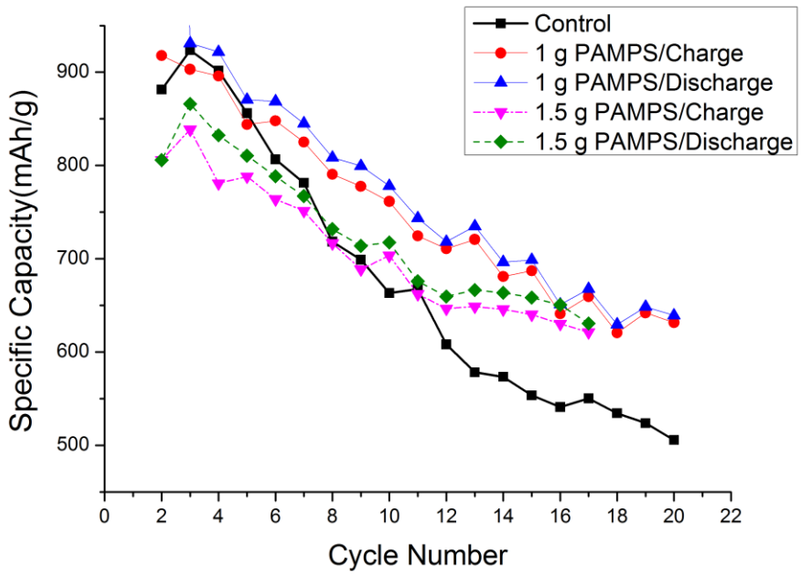

Figure 22 Comparison of cycling retention of control sample (Sn/PPy) without PAMPS and samples with PAMPS (Sn/PPy/PAMPS) containing 1g and 1.5g PAMPS respectively.

Another parameter is the deposition to time interval. The significance of this unique parameter is, as mentioned previously, due to the electrical repulsion between the working electrode which has negative potential and the negative charged $PAMPS^-$ salt dissolved in the solution. The results of three different deposition–to-interval ratios are shown in Figure 23.

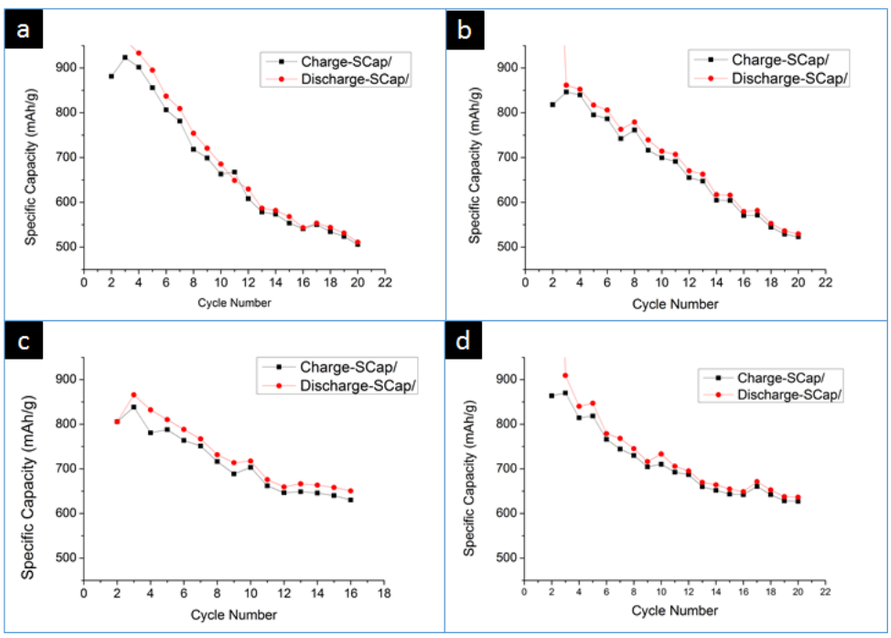

Figure 23 Cycling retention of a: control sample (Sn/PPy), b: sample made from 900s/0s deposition/interval ratio c: sample made from 50s/50s deposition/interval ratio, d: sample made from 25s/25s deposition/interval ratio.

The samples made from 25s and 50s intervals have better cycling retention than that made from continues 900s, while the difference between two ratios is not obvious. This proves that providing the intervals for the electrostatic attraction between PPy and PAMPS helps with the increase of PAMPS onto the film connecting with PPy. To make a clearer comparison, the cycling performances of control samples, PPy/Sn/PAMPS samples made from 50/50s deposition to interval ratio and PPy/Sn/PAMPS samples made from 25/25s deposition to interval ratio are shown in Figure 24. PPy/Sn/PAMPS samples made from 50/50s deposition/interval ratio have an eventual cycling retention about 78% after 20 cycles, compared to 57% of that of control samples, meaning the sufficient interval can provide the opportunity of the interaction between PPy and PAMPS. The network they formed will also improve the cycling retention due to the merits from the structure.

The differences of the cycling performances between samples made from 50/50s and 25/25s are not very distinguishable. So the exact interval that should be set still needs further investigation.

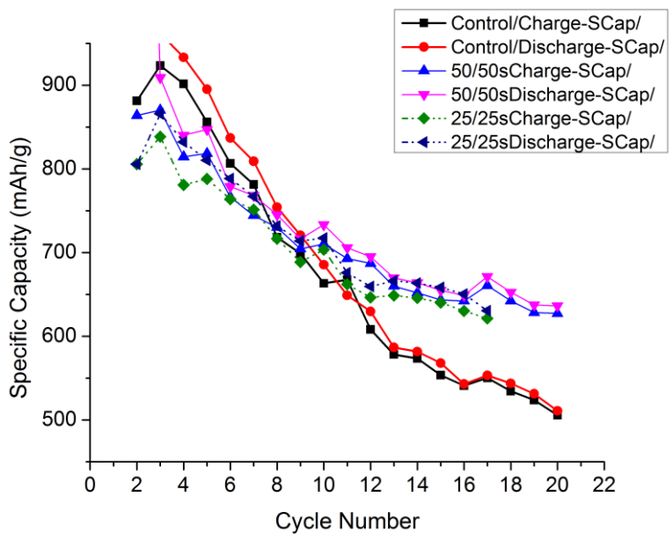

Figure 24 The comparison of cycling retention of control sample; PPy/Sn/PAMPS samples made from 50/50s depostion/interval ratio and PPy/Sn/PAMPS samples made from 25/25s depostion/interval ratio.

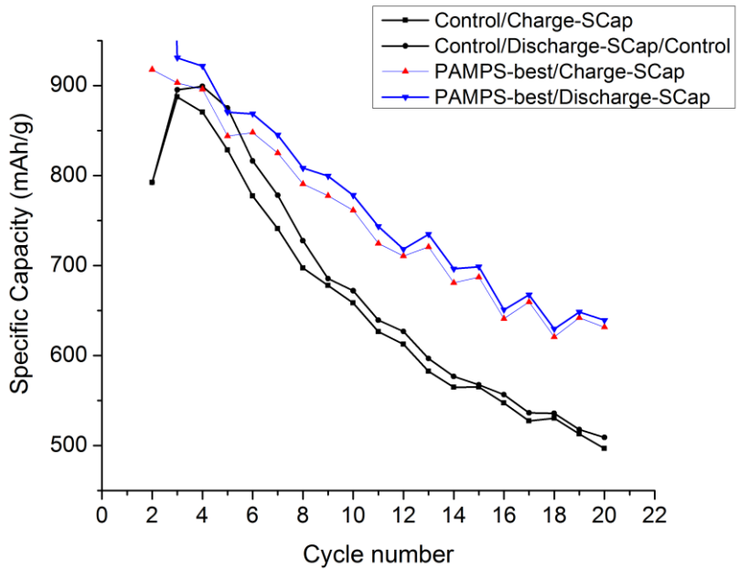

Figure 25 Cycling test comparison of best PPy/Sn/PAMPS sample and control sample.

Based on all of the cycling retention performances from each kind of samples, the final comparison of cycling retention test is shown in Figure 25, where PAMPS/Sn/PPy samples made using 1.5g PAMPS solution and under 50s/50s deposition to interval ratio time finally achieved 78% retention after 20 cycles compared to only 55% retention of control samples.

CHAPTER 5 CONCLUSION AND FUTURE WORK

In this dissertation, we introduce a conductive polymer-co-hydrogel binder incorporated with Sn nanoparticles as a newly generated lithium-ion battery anode to overcome the common issue of large volume expansion and pulverization during the charging and discharging process. The process is undergoing in situ onto the Cu surface and simultaneously by the electrochemical deposition in a 3-electrode cell. The advantage of electrochemical deposition method is that very thin film can be achieved and the thickness is controllable by adjusting the depositing parameters. Besides, EC deposition setup is quite convenient to assemble and the general experiment is much more straightforward and easier than chemical polymerization. Another novelty of the project is that Sn nanoparticles can be electrodeposited with conductive component at the same time onto the working electrode. This may be the only way so far using electrochemical deposition to fabricate the Sn-binder hybrid anode. This method can successfully make the anode using Sn as active material, whose specific capacity can achieve 923 $mAhg^{-1}$, approaching the theoretical capacity of Sn and almost 3 times higher than that of commercial graphite anode. From the SEM, TEM and EDX characterization, it reveals that a mesh-like porous network structure can be achieved, compared to the conventional anodically deposited PPy with a plain surface area. The mesh-porous architecture offers possible pathway for the transfer and diffusion of lithium ions between electrolyte and anode. Besides, the distribution of Sn nanoparticles is uniform on the thin film, occupying surface of PPy spheres. Hence PPy has function as buffer to decrease the volume expansion of Sn, and the capacity retention can be improved compared to pure tin anode.

The capacity retention is still poor after the incorporation of PPy, however, only remaining 54.7% after 20 cycles. To get further improvement, ideas about the conductive hydrogel are applied. One potential candidate is poly

(2-acrylamido-2-methyl-1-propanesulfonic acid) (PAMPS), which can serve as both crosslinker and doping anion for PPy because of its negative charged property after solving due to the existing of sulfuric acid groups. From SEM. TEM results, it is obvious that the contour of each PPy particles become less outstanding, meaning that PAMPS is encapsulating outside PPy and form an interpenetrating network by their electrostatic interaction.

From the cycling test, conclusion can be made that by increasing the amount of PAMPS solution, better cycle retention is achieved. This is because the overall amount of PAMPS hydrogel in the thin film is increasing. To investigate the influence of repulsion between working electrode applied with negative potential and negative charged PAMPS in solvent, three different deposition-to-interval ratios are selected for comparison. And from the cycling test results, samples made from processes with 50s and 25s intervals have better retention than that with no intervals. This suggested that the existing of intervals will benefit the attraction between PPy and PAMPS. Eventually, system made from the addition of 1.5g PAMPS and 50s intervals can achieve the best retention about 80% after 20 cycles. But compared to recent researches about the optimization of lithium-ion battery anode, these results are far from satisfaction. Much more efforts are needed.

So in the future, we plan to optimize the parameters of the PPy/Sn/PAMPS system. The PAMPS amounts, interval ratios and other deposition parameters are needed to be considered. Phytic acid is also an excellent choice and evenly better than the merit of PAMPS. But phytic acid can react with Sn ions in the solution and generate precipitates. Finding the solution to prevent their reaction is the first key point to allow the introduction of Phytic acid. If this can be solved, a dual hydrogel component network is achievable by combining Phytic acid and PAMPS. Besides, chemical polymerization methods are also promising and the systems in this project are also feasible by using

chemical polymerization. By integrating those future works we hope to achieve at least 90% retention after several hundred cycles.

REFERENCES

[1] Tarascon, J-M., and Michel Armand. "Issues and challenges facing rechargeable lithium batteries." Nature 414.6861 (2001): 359-367.

[2] Bruce, Peter G., Bruno Scrosati, and Jean-Marie Tarascon. "Nanomaterials for rechargeable lithium batteries." Angewandte Chemie International Edition47.16 (2008): 2930-2946.

[3] Su, Xin, *et al*. "Silicon-based nanomaterials for lithium-ion batteries: a review." Advanced Energy Materials 4.1 (2014): 1-23.

[4] Guiseppi-Elie, Anthony. "Electroconductive hydrogels: synthesis, characterization and biomedical applications." Biomaterials 31.10 (2010): 2701-2716.

[5] Rivero, Rebeca E., *et al*. "Pressure and microwave sensors/actuators based on smart hydrogel/conductive polymer nanocomposite." Sensors and Actuators B: Chemical 190 (2014): 270-278.

[6] Wu, Hui, *et al*. "Stable Li-ion battery anodes by in-situ polymerization of conducting hydrogel to conformally coat silicon nanoparticles." Nature communications 4 (2013): 1-6.

[7] Winter, Martin, and Jürgen O. Besenhard. "Electrochemical lithiation of tin and tin-based intermetallics and composites." Electrochimica Acta 45.1 (1999): 31-50.

[8] R. A. Huggins in Lithium Batteries (Eds.: G.-A. Nazri, G. P. (2004). Kuwer Academic, Boston, 270.

[9] Aricò, Antonino Salvatore, *et al*. "Nanostructured materials for advanced energy conversion and storage devices." Nature materials 4.5 (2005): 366-377.

[10] Magasinski, Alexandre, *et al*. "Toward efficient binders for Li-ion battery Si-based anodes: polyacrylic acid." ACS applied materials & interfaces 2.11 (2010): 3004-3010.

[11] Mazouzi, D., Lestriez, B., Roue, L., & Guyomard, D. (2009). Silicon composite electrode with high capacity and long cycle life. Electrochemical and Solid-State Letters, 12(11), A215-A218.

[12] Chen, Zonghai, L. Christensen, and J. R. Dahn. "Large-volume-change electrodes for Li-ion batteries of amorphous alloy particles held by elastomeric tethers." Electrochemistry communications 5.11 (2003): 919-923.

[13] Bao, Zhihao, *et al*. "Chemical reduction of three-dimensional silica micro-assemblies into microporous silicon replicas." Nature 446.7132 (2007): 172-175.

[14] Kovalenko, Igor, *et al.* "A major constituent of brown algae for use in high-capacity Li-ion batteries." Science 334.6052 (2011): 75-79.

[15] Pan, L., Qiu, H., Dou, C., Li, Y., Pu, L., Xu, J., & Shi, Y. (2010). Conducting polymer nanostructures: template synthesis and applications in energy storage. International journal of molecular sciences, 11(7), 2636-2657.

[16] Liu, B., Soares, P., Checkles, C., Zhao, Y., & Yu, G. (2013). Three-dimensional hierarchical ternary nanostructures for high-performance Li-ion battery anodes. Nano letters, 13(7), 3414-3419.

[17] Jung, Y., Singh, N., & Choi, K. S. (2009). Cathodic Deposition of Polypyrrole Enabling the One-Step Assembly of Metal–Polymer Hybrid Electrodes. Angewandte Chemie International Edition, 48(44), 8331-8334.

[18] Green, R. A., Hassarati, R. T., Goding, J. A., Baek, S., Lovell, N. H., Martens, P. J., & Poole-Warren, L. A. (2012). Conductive hydrogels: mechanically robust hybrids for use as biomaterials. Macromolecular bioscience, 12(4), 494-501.

[19] Mahloniya, R. G., Bajpai, J., & Bajpai, A. K. (2012). Electrical actuation of ionic hydrogels based on polyvinyl alcohol grafted with poly (2-acrylamido-2-methyl-1-propanesulfonic acid-co-acrylonitrile) chains. Polymer Composites, 33(1), 129-137.

[20] Li, Yongfang, and Jing Yang. "Effect of electrolyte concentration on the properties of the electropolymerized polypyrrole films." Journal of applied polymer science 65.13 (1997): 2739-2744.

[21] Holleman, A. F.; Wiberg, E. (2001), Inorganic Chemistry, San Diego: Academic Press.

[22] D. L. H. Williams, Nitrosation, Cambridge University Press, Cambridge, 1988.

[23] Von G. A. Olah, R. Malhotra und S. C. Narang. VCH Verlagsgesellschaft, Weinheim/VCH Publishers, New York 1989.

[24] O.W. J. S. Rutten, A. Van Sandwijk, G. Van Weert, J. Appl. Electrochem. 1999, 29, 87 – 92.

[25] M. Pourbaix, Atlas of Electrochemical Equilibria in Aqueous Solutions, 2nd ed., National Association of Corrosion Engineers, Houston, 1974, p. 384.

[26] Pan, Lijia, *et al*. "Hierarchical nanostructured conducting polymer hydrogel with high electrochemical activity." Proceedings of the National Academy of Sciences 109.24 (2012): 9287-9292.

[27] Wu, Ping, *et al*. "Carbon-coated SnO_2 nanotubes: template-engaged synthesis and their application in lithium-ion batteries." Nanoscale 3.2 (2011): 746-750.